



Compromised alveolar bone cells in a patient with dentinogenesis imperfecta caused by *DSPP* mutation

Thanrira Porntaveetus^{1,2}  · Nunthawan Nowwarote³ · Thanaphum Osathanon^{1,3} · Thanakorn Theerapanon¹ · Prasit Pavasant³ · Lawan Boonprakong⁴ · Kittisak Sanon⁵ · Sirivimol Srisawasdi⁵ · Kanya Suphapeetiporn^{6,7} · Vorasuk Shotelersuk^{6,7}

Received: 20 October 2017 / Accepted: 9 April 2018
© Springer-Verlag GmbH Germany, part of Springer Nature 2018

Abstract

Objectives Dentin sialophosphoprotein (*DSPP*) plays an important role in the mineralization of both dentin and bones. The *Dspp* null mice developed periodontal diseases. Patients with *DSPP* mutations have dentinogenesis imperfecta (DGI), but very little is known about their bone characteristics. This study aims to characterize alveolar bone cells of a DGI patient with *DSPP* mutation.

Materials and methods Pathogenic variants were identified by whole exome and sanger sequencing. Cells isolated from the alveolar bones of a *DSPP* patient were investigated for their characteristics including cell morphology, attachment, spreading, proliferation, colony formation, mineralization, and osteogenic differentiation.

Results We identified a Thai family with three members affected with autosomal dominant DGI harboring a heterozygous pathogenic missense mutation, c.50C>T, p.P17L, in exon 2 of the *DSPP* gene. The patients' phenotypes presented deteriorated opalescent teeth with periapical lesions, thickening of lamina dura, furcation involvement, alveolar bone loss, and bone exostoses. The alveolar bone cells isolated from *DSPP* patient exhibited compromised proliferation and colony formation. Scanning electron microscope revealed altered cellular morphology and spreading. The *DSPP* cells showed deviated *mRNA* levels of *OCN*, *ALP*, and *COL1* but maintained in vitro mineralization ability compared to the control.

Conclusions We demonstrate that the *DSPP* p.P17L mutant alveolar bone cells had compromised cell spreading, proliferation, colony formation, and osteogenic induction, suggesting abnormal bone characteristics in the patient with DGI caused by *DSPP* mutation.

Clinical relevance *DSPP* mutation can induce the behavior alterations of alveolar bone cells.

Keywords Bone biology · Cell biology · Diagnosis · Genetics · Osteoblasts

Electronic supplementary material The online version of this article (<https://doi.org/10.1007/s00784-018-2437-7>) contains supplementary material, which is available to authorized users.

✉ Thanrira Porntaveetus
thanrira.p@chula.ac.th

¹ Craniofacial Genetics and Stem Cells Research Group, Faculty of Dentistry, Chulalongkorn University, Bangkok 10330, Thailand

² Department of Physiology, Faculty of Dentistry, Chulalongkorn University, Bangkok 10330, Thailand

³ Excellence Center in Regenerative Dentistry and Department of Anatomy, Faculty of Dentistry, Chulalongkorn University, Bangkok 10330, Thailand

⁴ Oral Biology Research Center, Faculty of Dentistry, Chulalongkorn University, Bangkok 10330, Thailand

⁵ Department of Operative Dentistry, Faculty of Dentistry, Chulalongkorn University, Bangkok 10330, Thailand

⁶ Center of Excellence for Medical Genetics, Department of Pediatrics, Faculty of Medicine, Chulalongkorn University, Bangkok 10330, Thailand

⁷ Excellence Center for Medical Genetics, King Chulalongkorn Memorial Hospital, the Thai Red Cross Society, Bangkok 10330, Thailand

Introduction

The *DSPP* gene encodes a member of the small integrin-binding ligand N-linked glycoproteins (SIBLINGS) [1]. Its encoded protein, DSPP (dentin sialophosphoprotein), is cleaved into dentin sialoprotein (DSP) and dentin phosphoprotein (DPP), which have distinct functions in dentin mineralization [1]. The *DSPP* gene consists of five exons locating on chromosome 4q22.1 [2]. Human mutation in *DSPP* is associated with non-syndromic dentinogenesis imperfecta and dentin dysplasia [3, 4]. In addition to odontoblasts and dentin, osteoblasts and bones also highly express *DSPP* [5, 6].

Mineral deposition defects were observed in alveolar and cranial bones in *Dspp* null mice [7]. The null mice showed a significant loss of alveolar bone and cementum, particularly in the furcation and interproximal areas of the molars, resulting in periodontal diseases [8, 9]. In femur, *Dspp* null mice exhibited lower bone volume fraction, trabecular number, and mineral density, as well as the decrease of crystallinity [10]. Calvarial cells isolated from the *Dspp* null mice showed decreased mineralization in vitro corresponding with the reduced *Runx2*, *Osx*, *Coll1*, and *OPN* mRNA levels compared to control cells [7]. *DSPP* knockdown in human dental pulp stem cells significantly disturbed the mineral formation [11].

It was reported that the DSP domain promoted an attachment and spreading of murine dental papilla mesenchymal cells by its binding to integrin $\beta 6$ receptor [12]. The actin polymerization occurring upon integrin activation was shown to participate in osteogenic differentiation [13]. Hence, DSP regulating actin cytoskeletal could participate in the influence of DSPP on odonto/osteogenic differentiation.

Previous evidences have demonstrated that *DSPP* plays a crucial role in hard tissue metabolism especially mineralization. *DSPP* mutations obviously disturb dentin formation. Yet, the characteristics of alveolar bone cells in *DSPP* patients have not been previously explored. We hypothesized that *DSPP* mutation could lead to the dysfunction of osteoblasts and alter the periodontium features observed in our patient. Our study identified DGI patients with a hot spot mutation in the *DSPP* gene. The *DSPP* alveolar bone cells were investigated for their behaviors including cell morphology, proliferation, colony formation, attachment, spreading, mineralization, and osteogenic marker expression compared with the cells from control donors.

Materials and methods

Subject enrollment

A Thai family with three members affected with isolated DGI was recruited. The study was exempted from review by the Institutional Review Board, Faculty of Medicine,

Chulalongkorn University (IRB No. 469/60) and performed in accordance with the ethical standards as laid down in the 1964 Declaration of Helsinki and its later amendments or comparable ethical standards. Written informed consent was obtained from all participants.

DNA isolation and whole exome sequencing (WES)

Blood samples were collected from the proband and her family members. The genomic DNA was extracted from peripheral blood leukocytes of the proband's affected son and sent to MacroGen, Inc. (Seoul, Korea). The DNA sample was prepared according to previous publication [14]. Variant calling was performed using GATK with HaplotypeCaller. Finally, SNVs and Indels were annotated by using SnpEff and annotation databases, dbpSNP142, 1000 Genome, ClinVar, and ESP. All SNVs and Indel were first filtered by known genes causing DGI. They were subsequently discarded if present in our in-house database of 700 unrelated Thai exomes. The variants would be called novel if they were not listed in the Human Gene Mutation Database (www.hgmd.cf.ac.uk/ac/index.php) and the Exome Aggregation Consortium database (exac.broadinstitute.org).

Sanger sequencing

The variants were confirmed by PCR and Sanger sequencing. The PCR products were treated with ExoSAP-IT (USP Corporation, Cleveland, OH) and sent for direct sequencing at MacroGen. Sequence data were analyzed using Sequencher (V.5.0; Gene Codes Corporation, Ann Arbor, MI). Primer sequences were shown in Supplementary Table.

Cell isolation and culture

After alveolectomy, bone chips were washed with sterile PBS, minced into small pieces, cleaned of adherent soft tissue, rinsed, and placed into 35-mm tissue culture dishes. Explanted cells were maintained in Dulbecco's Modified Eagle Medium (DMEM; Gibco BRL, Carlsbad, CA, USA) containing 10% FBS, 2-mM L-glutamine, 100-U/mL penicillin, 100-mg/mL streptomycin, and 250-ng/mL amphotericin B in 100% humidity, 37 °C, and 5% carbon dioxide. Medium was changed once every 48 h. Upon confluence, cells were subcultured using trypsin/EDTA solution and named as passage 1. The cells with similar passage isolated from healthy individuals whom underwent surgical alveolar bone excision according to normal treatment plan (i.e., bone exostosis) were used as the controls.

Cell proliferation and colony forming unit assay

Cell proliferation was assessed by MTT assay [15]. Cells were seeded at density of 12,500 cells per well in 24-well plate. At designated time point, cells were incubated with 0.5-mg/ml 3-(4,5-dimethylthiazol-2-yl)-2,5-diphenyltetrazolium bromide solution (USB Corporation) for 30 min. Precipitated formazan crystals were solubilized in dimethylsulfoxide and glycine buffer. The absorbance was measured at 570 nm. For colony forming unit assay, cells were seeded at density of 500 cells per well in 60-mm tissue culture plate and maintained in growth medium for 14 days [15]. Colonies were fixed with 4% buffered formalin for 10 min and stained with Coomassie blue solution.

Mineralization assay

Cells were seeded at density of 50,000 cells per well in 24-well plate and maintained in osteogenic induction medium, which consisted of growth medium supplemented with 50- μ g/ml ascorbic acid (Sigma-Aldrich Chemical, St. Louis, MO, USA), 250-nM dexamethasone (Sigma-Aldrich Chemical), and 5-mM β -glycerophosphate (Sigma-Aldrich Chemical). At day 14, cells were fixed with cold methanol and rinsed with deionized water. Calcium deposition was determined by staining with 1% Alizarin Red S solution for 3 min at room temperature.

Real-time polymerase chain reaction

Total cellular RNA was isolated using RiboEx total RNA isolation solution (GeneAll, Seoul, South Korea). The amount and integrity of isolated RNA were evaluated using Nanodrop. One microgram of RNA was converted to complementary DNA using a reverse transcriptase reaction (ImPromII kit, Promega, Madison, WI, USA). Real-time polymerase chain reaction was performed with SYBR green detection system (FastStart Essential DNA Green Master, Roche Diagnostic, USA) on MiniOpticon real-time PCR system (Bio-Rad, USA). Melt-curve analysis was performed to determine product specificity. The expression value was normalized to *18S* expression value and further normalized to the control. Primer sequences were shown in Supplementary Table.

Cell attachment and spreading assay

Cells were seeded at density of 12,500 cells per well in 24-well plate and maintained in growth medium. At designated time points, cells were fixed with 2.5% glutaraldehyde (Sigma-Aldrich Chemical) in PBS for 30 min, dehydrated, and gold sputter coated. Cell morphology was evaluated using scanning electron microscope (SEM, Quanta 250, FEI,

Hillsboro, OR, USA). To determine cell spreading, cells were categorized into four groups according to the criteria previously reported [16–18]. Round cells with/without few filopodia were assigned as stage 1. Cells with numerous cytoplasmic extension were categorized as stage 2. Circumferential extension of lamellopodia with dome-like center morphology was assigned as stage 3 and flattened and fully spreaded cells were categorized as stage 4. Percentage of cells in each stage per field ($\times 500$ magnification) was calculated. Cytoskeleton arrangement was examined by the phalloidin immunocytochemistry staining (rhodamine-phalloidin, Invitrogen, USA), and the nuclei were counterstained with DAPI.

Statistical analyses

For each donor, the experiments were performed in quadruplicate ($n = 4$). For two group comparison, Mann-Whitney *U* test was employed. Kruskal-Wallis test following by a pairwise comparison (Dunn-Bonferroni approach) was performed in three- or more-group comparison. All statistical analysis was examined by IBM SPSS Statistics for Mac, Version 22 (Armonk, NY, USA). The statistical significance was considered at $p < 0.05$.

Results

Manifestation and management of DGI

The proband at 38 years of age presented for dental treatment at the Faculty of Dentistry, Chulalongkorn University. She had eating and esthetic problems. Oral examination revealed that all of her teeth exhibited extreme wear and fracture leaving multiple retained roots with brown opalescent appearance. Multiple teeth were clinically absent. Her dental arch had severe atrophy in the edentulous areas and numerous bone exostoses (Fig. 1a–c). Dental radiographs showed short root, bulbous crown, pulp obliteration, periapical lesions, thickening of lamina dura, bone sclerosis between the lamina dura of adjacent teeth, and alveolar bone loss. All mandibular teeth developed pulp necrosis with asymptomatic apical periodontitis, which were later extracted (Fig. 1d–j). Alveolectomy was performed to reshape the mandibular arch (Fig. 1k, l). The maxillary teeth were in fair condition without any symptoms. The maxillary overdenture and mandibular complete denture were delivered for the patient (Fig. 1m–o). Her father and son were also affected with DGI (Fig. 1p). Her son presented for dental treatment at 7 years of age. His mixed dentition exhibited opalescent teeth with severe attrition. The edentulous areas exhibited severe bone atrophy (Fig. 2a–c). The primary maxillary first molars and right canine and mandibular second molars were missing. His gingiva appeared darkened. Dental

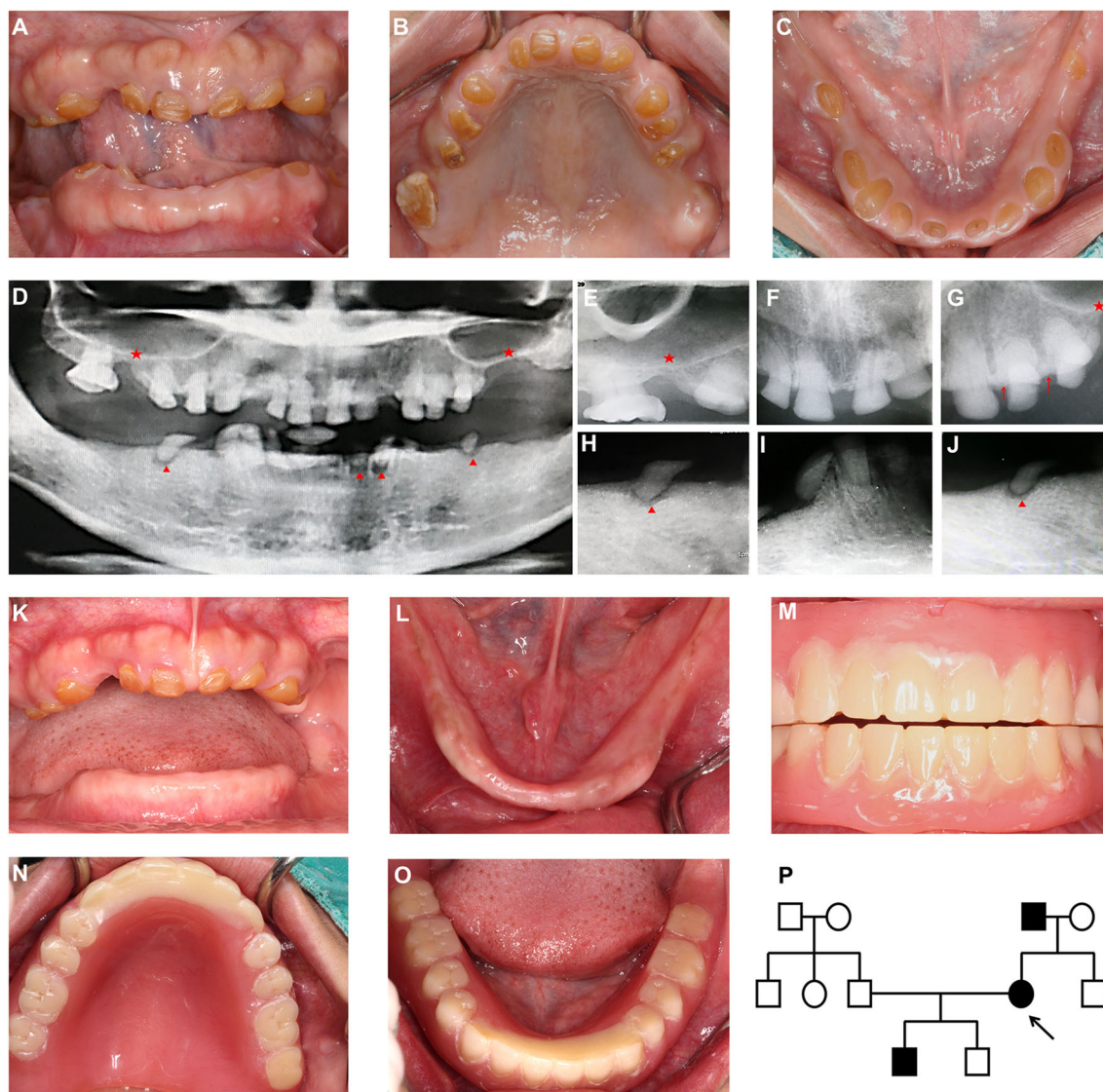


Fig. 1 Clinical and radiographic manifestations of the proband and pedigree of the family. **a–c** Frontal, maxillary, and mandibular clinical photographs of the proband at 38 years of age showed opalescent teeth with severe attrition. The dental arches showed numerous bone exostoses and severe alveolar bone atrophy in the edentulous areas. **d–j** Panoramic and periapical radiographs revealed bulbous crowns, pulp obliteration, several periapical lesions (arrowheads), thickened lamina dura, bone sclerosis between the lamina dura of adjacent teeth (arrows), and

alveolar bone loss (stars). **k, l** Frontal and mandibular clinical photographs of the dental arch after mandibular alveolectomy and alveoloplasty. **m–o** Frontal, maxillary, and mandibular photographs of upper overdenture and lower complete denture. **p** Diagram demonstrates the pedigree of the proband's family. The blackened symbols represent the clinically affected individual. The arrow indicates proband

radiographs revealed the permanent anterior teeth with pulp cavities, first molar with pulp obliteration, and erupting second molars with taurodontism. The widened periodontal ligament (PDL) space especially at the crest of the furcation was observed in the molars at age 8 years (Fig. 2d–h). All permanent first molars were initially restored with stainless steel crowns cemented with glass ionomer cement. However, the crowns were later embedded in the gingiva after 1-year of placement. The gingivectomy using electrosurgery was then performed at the distal gingival margin of the permanent first molars. The first molars were built up with Build it® (Pentron,

CA, USA) using All-bond 3® adhesive (Bisco Dental, Illinois, USA). The teeth were restored with palladium crowns bonded with C&B™ cement (Bisco Dental, Illinois, USA). The patient's vertical dimension was reestablished to provide the space for the restorations of anterior teeth. Noticeably, these teeth at age 10 years showed wider PDL space and furcation involvement. No calculus was shown in the radiographs (Fig. 2i–k). All permanent incisors were restored with resin composite bonded with OptiBond™ FL adhesive (Kerr, CA, USA). Nance holding arch and lingual arch were placed to maintain arch space (Fig. 2l–n). The crowns crown of the

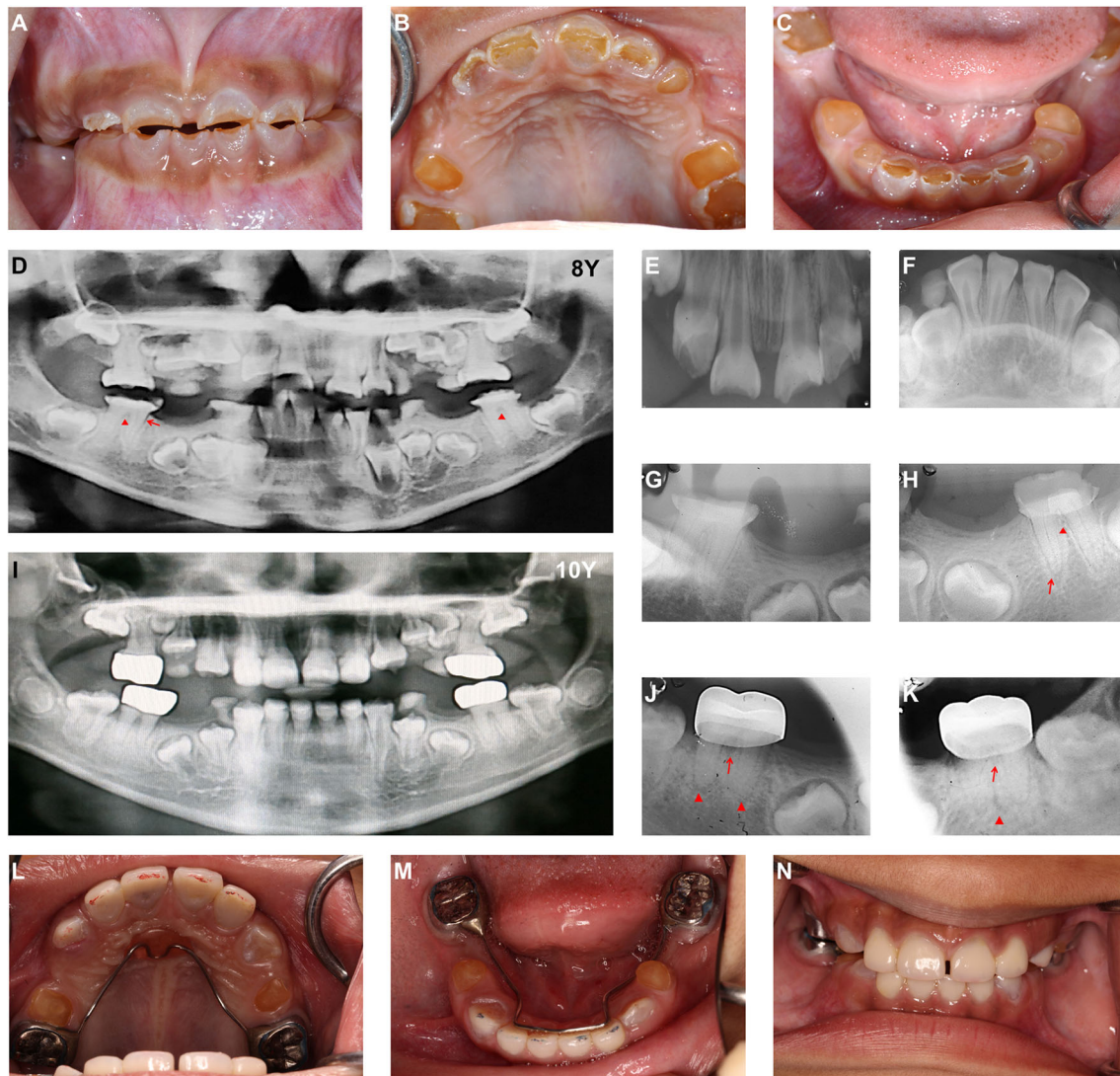


Fig. 2 Clinical and radiographic manifestations of the proband's son. **a–c** Frontal, maxillary, and mandibular clinical photographs of the affected son at the age of 8 years showed opalescent teeth with severe attrition and multiple missing teeth. The edentulous areas were hypoplastic. **d–h** Panoramic and periapical radiographs at the age of 8 years exhibited short and bulbous crown, cervical constriction, various degrees of pulp

obliteration, widening of PDL space (arrows), thickened lamina dura, and furcation involvement (arrowheads). **i–k** At 10 years of age, the first molars showed wider PDL space, furcation involvement (arrows), and periapical lesions (arrowheads). **l–n** The permanent first molars were restored with palladium crowns and the anterior teeth with resin composite. Space maintainers were delivered

mandibular right first molar (LR6) were dislodged twice in 6 months. The tooth had periapical lesions and was negative to electrical pulp test and positive to percussion and palpation indicating asymptomatic irreversible pulpitis with symptomatic apical periodontitis (Supplementary Figure). Periodic recall was implemented to monitor and reevaluate patients' dental and periodontal health.

Identification of *DSPP* mutation

WES revealed heterozygous missense mutation, c.50C > T, p.P17L, in the exon 2 of the *DSPP* gene (NM_014208.3), suggesting that DGI in this family was inherited in an autosomal dominant manner. The variant was co-segregated in her father

and son, but not present in unaffected family members (Fig. 3a, b). The mutation resulted in a substitution of a proline to leucine at the second codon of the DSP domain (Fig. 3c). This position is highly conserved among several species including human (NP_055023.2), chimpanzee (XP_016807336.1), mouse (NP_034210.2), rat (NP_036922.2), cattle (XP_002688455.1), and frog (XP_012813201.1) (Fig. 3d).

Compromised cell proliferation and osteogenic marker gene expression

Cells from the alveolar bone of a *DSPP* mutation patient were isolated and characterized compared with those isolated from healthy donors. Cells from both the *DSPP* mutant and the

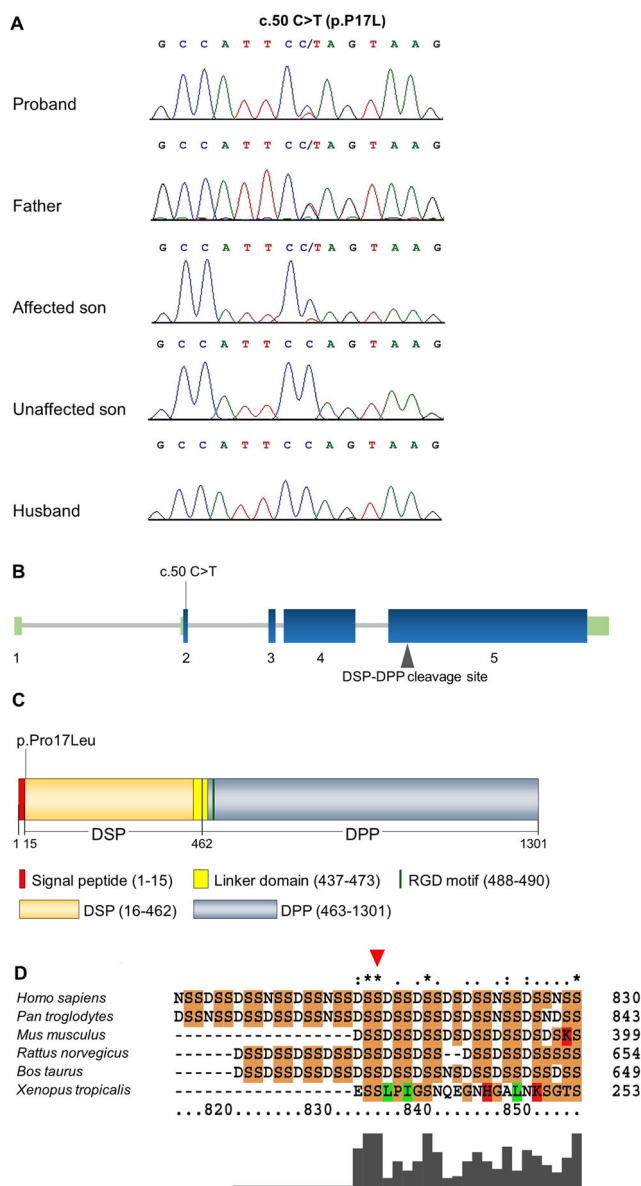


Fig. 3 Genetic analyses of the proband's family. **a** An electropherogram demonstrated a heterozygous mutation, c.50C > T (p.P17L), in the exon 2 of the *DSPP* gene (NM_014208.3) in the proband. The mutation was observed in her father and affected son. **b** The mutation was located in the exon 2 of the *DSPP* gene. **c** The amino acid was altered in the DSP domain (NP_055023.2). **d** Sequence alignment of partial amino acid sequence of DSPP. Conservation of the proline¹⁷ across species is indicated by red arrowhead

control donors were able to proliferate, as the number of cells was significantly increased at day 7 compared with day 1 ($p = 0.029$). However, no significant increase of cell number was observed in *DSPP* mutant cells at day 3 ($p = 0.114$), while the significant increase of cell number was detected in the control cells ($p = 0.029$) (Fig. 4a). Colonies formed by *DSPP* mutant cells exhibited slightly lower in number compared with the control cells (Fig. 4b). After maintained in osteogenic induction medium for 14 days, the marked increase of mineral

deposition was noted in mutant cells similar to those of the control (Fig. 4c). Interestingly, mutant cells did not upregulate *ALP* mRNA expression ($p = 0.343$), while cells from the control donors exhibited the significant increase of *ALP* levels at day 7 compared to day 3 in osteogenic induction condition ($p = 0.029$) (Fig. 4d). Interestingly, the *DSPP* mutant alveolar bone cells exhibited significantly decreased *OCN* mRNA levels compared with the control at day 7 ($p = 0.029$) (Fig. 4e). However, the control cells did not exhibit dramatic change in *OCN* mRNA levels after osteogenic induction for 7 days (donor 1 $p = 0.343$; donor 2 $p = 0.343$; donor 3 $p = 1.000$) (Fig. 4e). The upregulation of *RUNX2* was observed ($p = 0.029$), while *COL1* mRNA levels remained unchanged at day 7 in *DSPP* mutant alveolar bone cells ($p = 0.343$) (Fig. 4f, g).

Delayed cell spreading

Cell morphology was determined by SEM analysis and F-actin staining. For mutant cells, cell attachment on tissue culture surface was observed as early as 30 min after seeding (Fig. 5a). Lamellopodia formation was noted at 2 h, and fully cell spreading was detected at 6 and 24 h (Fig. 5b–d). In the control cells, a marked filopodia and lamellopodia cytoplasmic extension was evidenced at 30 min after seeding (Fig. 5e, f). Cell spreading was categorized into four stages. Cells in stage 1 exhibited round in shape, and a few filopodia extension might be observed (Fig. 5i). Cells with numerous cytoplasmic extension were categorized as stage 2 (Fig. 5j). Circumferential extension of lamellopodia with dome-like center morphology, and flatted and fully spread cells were categorized as stages 3 and 4, respectively (Fig. 5k, l). The quantitative cell count in each spreading stage demonstrated that percentage of cells in stage 1 was significantly higher in mutant cells than cells from other donors at 30 min ($p = 0.001$) and 2 h ($p = 0.001$) (Fig. 5m, n).

F-Actin orientation was examined using phalloidin immunocytochemistry staining. Stress fibers of actin were clearly noted in the control cells at 2 h, while the actin fibers in mutant cells were not organized. At 6 h, stress fibers were obviously observed in both mutant and the control cells. At 24 h, mutant cells exhibited thin parallel actin fibers, while the control cells generally had thicker bundle of actin filaments (Fig. 5o–v).

Discussion

The present study described a Thai family with three members affected with an autosomal dominant DGI. Their oro-dental phenotypes include defective dentin and periodontium. Cells isolated from the proband's alveolar bone demonstrated decreased cell proliferation and colony forming unit, delayed cell spreading, as well as down-regulation of *OCN* upon osteogenic differentiation.

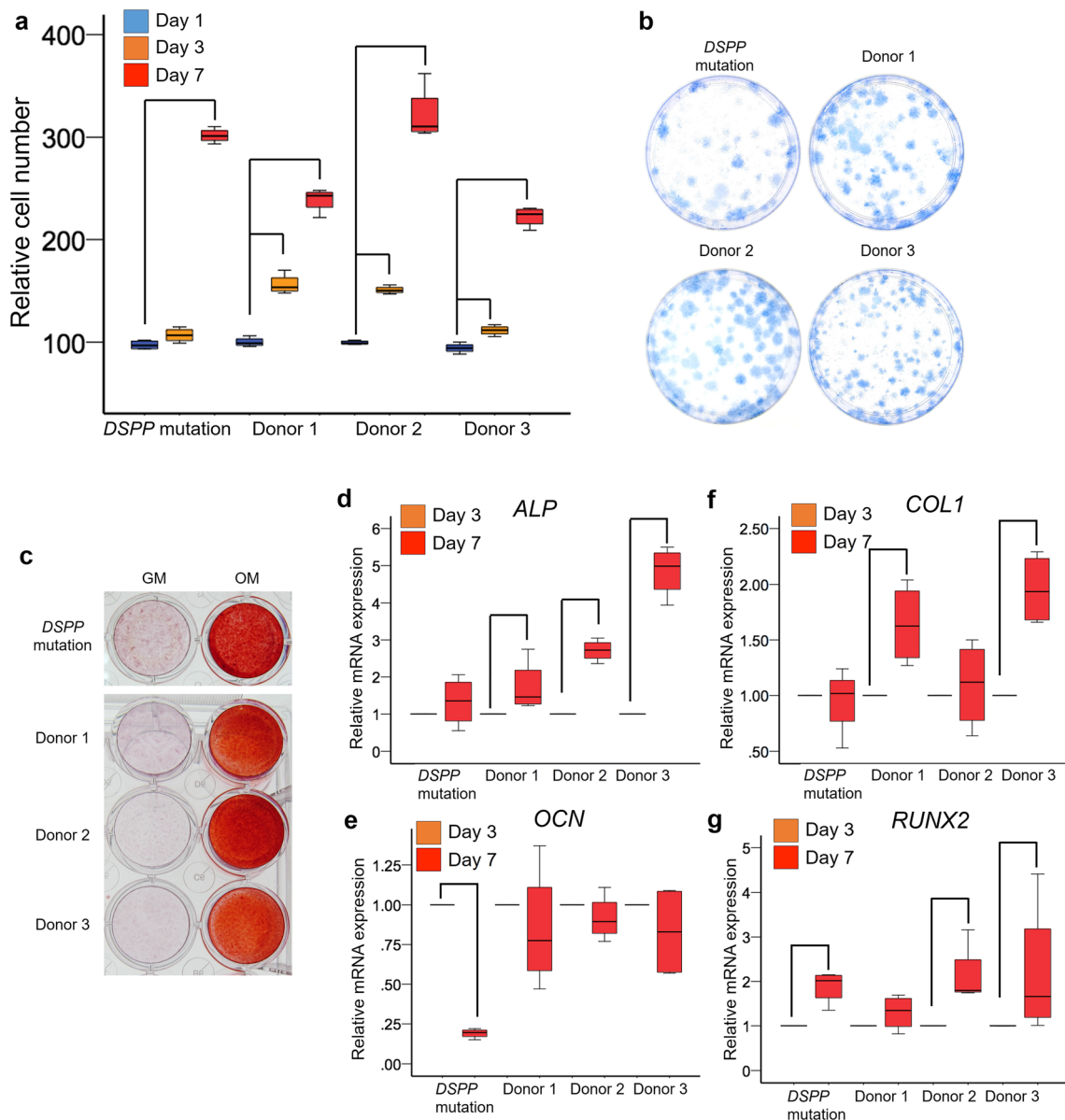


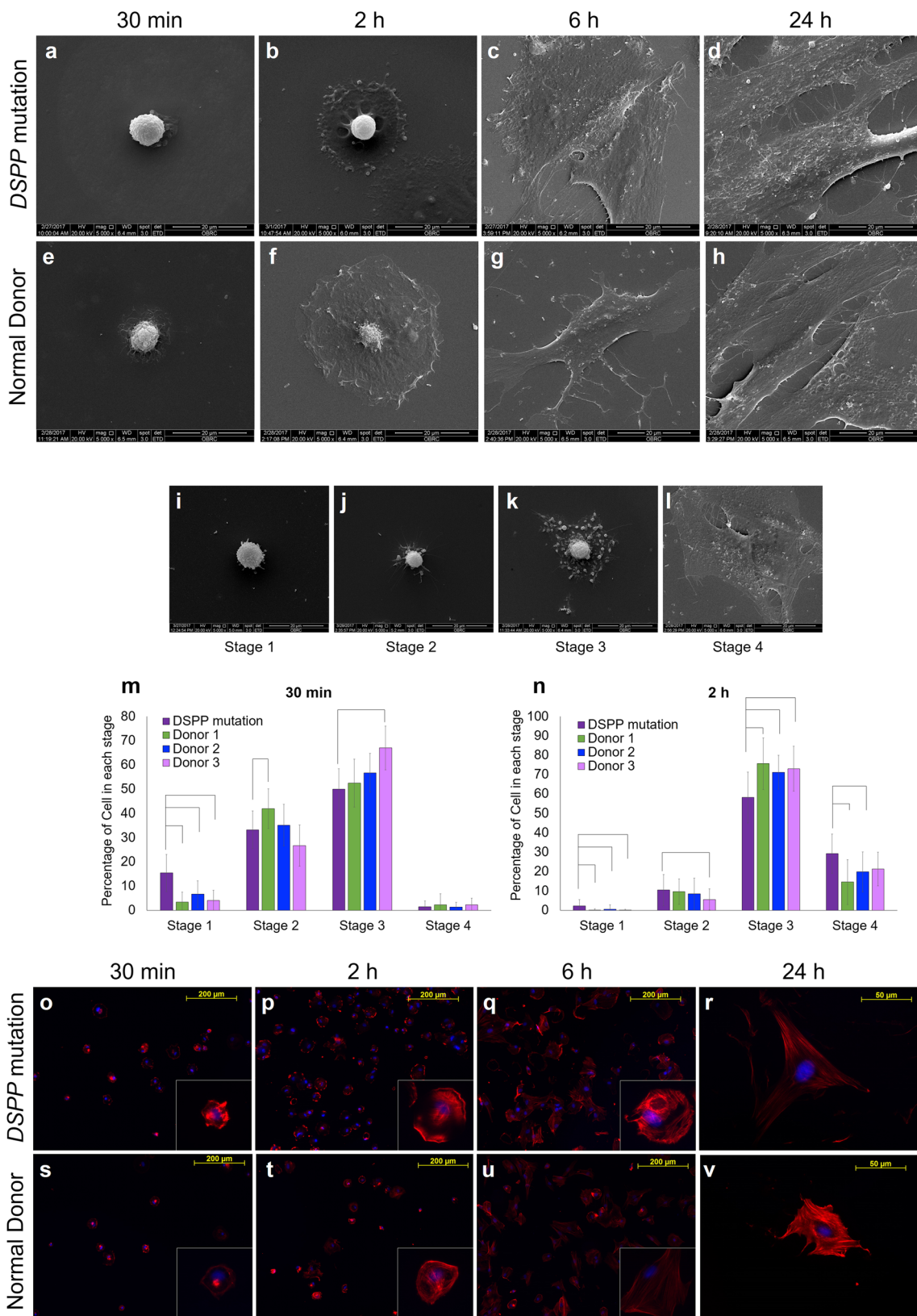
Fig. 4 Cell proliferation and osteogenic marker gene expression characteristics of *DSPP* mutant alveolar bone cells. **a** Box and whisker plot demonstrated cell viability evaluating by MTT assay and a relative cell number was calculated from the absorbance of solubilized formazan crystals. **b** Colony forming unit ability was assessed after maintaining cells in growth medium for 14 days. **c** Cells were maintained in

osteogenic induction medium for 14 days and an in vitro mineral deposition was determined using Alizarin Red S staining. **d–g** Box and whisker plots demonstrated an osteogenic marker gene expression, determined using real-time polymerase chain reaction. Bars indicated the statistically significant difference ($p < 0.05$)

The affected patients exhibited a mutation, c.50C > T, p.P17L, in the *DSPP* gene. The mutation was located in the exon 2 at the second nucleotide of the last codon and the second amino acid of the DSP domain. This mutation was previously identified in a Chinese family with DGI type II and a Korean family with DGI type III [19, 20]. DGI types II and III are not associated with osteogenesis imperfecta. The p.P17T (c.49C > A) mutation was previously associated with DGI and bilateral progressive high-frequency sensorineural hearing loss [21]. However, hearing loss is not observed in our patients. In addition, the p.P17S (c.49C > T) variant was

formerly associated with DGI types II and III [22, 23]. Recent genetic studies showed that type II and III categories are severity variations of the same disease [24]. The variant identified in the present study is the six disease-causing mutation affecting the *DSPP* P17 residue associated with DGI. This, together with the evolutionary conservation of the P17 residue, supports that this is a mutational hot spot and important for the function of *DSPP*.

Cells isolated from human mandibular bone were shown to contain stem cell subpopulation. The STRO-1⁺ mandibular cells exhibited mesenchymal stem cell markers and



multipotential differentiation ability [25]. The present study employed heterogeneous cells isolated from alveolar bone. These cells were expressed osteoblast related genes and were

able to mineralize after maintained in osteogenic medium. Similarly, heterogeneous cells isolated from human alveolar bone demonstrated the ability of proliferation in vitro and

◀ **Fig. 5** Cell morphology and cell spreading property of *DSPP* mutant alveolar bone cells. **a–h** Cells were seeded on tissue culture plate for 30 min, 2, 6, and 24 h. Representative micrographs of *DSPP* mutant alveolar bone cells (**a–d**) and the control donor (**e–h**) illustrated the cell morphology at different time point after seeding. **i–l** Characteristics of cell spreading in stages 1 to 4 were demonstrated. **m, n** Cells in each stage at 30 min and 2 h were counted and presented as percentage of cells per field ($\times 500$). Bars indicated the statistically significant difference ($p < 0.05$). **o–v** Cells seeded on tissue culture plate for 30 min, 2, 6, and 24 h showed F-actin orientation during cell attachment and spreading. F-Actin was stained with rhodamine-phalloidin

exhibited osteoblast marker genes, namely *ALP*, *OPN*, and *OCN*. These cells showed an increased mineral deposition upon cultured in osteogenic medium [23]. Although, we could not imply that cells employed in the present study were progenitor cells. These cells exhibited osteoblast-like phenotypes, which may be used as the representative cells from alveolar bone.

The expression of *DSPP* was observed in the alveolar bone cells [5, 6]. Previous animal studies showed defective alveolar bone and periodontium in the *Dspp* null mice [7, 8]. The *Dmp1* knockout mice with significantly decreased *DSPP* expression exhibited defective tooth and alveolar bone, which were rescued by transgenic expression of *DSPP* [26]. Overexpression of N-terminal of *DSPP* aggravated alveolar bone loss in *Dspp* knockout mice [27]. Several molecular studies also demonstrated the important roles of *DSPP* in bone and dental cells. The DSP residues between amino acid 183 and 457 were shown to stimulate PDL stem cell proliferation and differentiation [28]. N-Terminal dentin sialoprotein (N-DSP) was shown to promote bone formation by accelerating osteoblast cell proliferation and differentiation and inducing the expression of osteogenic markers, such as *Col1*, *Runx2*, *Osterix*, and *ATF* [22]. The odontoblast-lineage cells transfected with N-terminal mutation in the DSP domain showed a mark decreases in ALP activity, and the expression of *Col1* and *Ocn* compared with cells transfected with mutations in the signal peptide region or in the C-terminal of DSP domain [29]. Our previous report demonstrated that in stem cells isolated from human exfoliated deciduous teeth from the patient with 4-bp deletion in the exon 5 of the *DSPP* gene, we observed defective periodontium in our patient. In this study, the p.P17L alveolar bone cells isolated from a DGI patient exhibited compromised cell spreading, cell proliferation, colony formation, and altered expressions of *ALP*, *OCN*, and *COL1*. Based on many lines of these evidences, it is suggested that *DSPP* is present and important in the alveolar bone cells, and alterations of alveolar bone cells' behaviors including proliferation and odonto/osteogenic differentiation could be influenced by specific mutation in the *DSPP* gene. Previous pathogenesis analysis revealed that the P17L mutation caused endoplasmic reticulum retention and defective protein secretion. It was expected to exert a dominant negative effect on *DSPP* function [20]. These suggest the possible mechanism involved in the alterations of p.P17L mutant alveolar bone cells.

Calvarial cells isolated from *Dspp*-null mice exhibited the significant reduction of *Runx2*, *Col1*, and *Opn* expression and mineralization [7]. In the present study, no significant difference in mineral deposition was observed in *DSPP* cells compared to the controls. Several explanations are hypothesized. First, cells isolated from calvarias, particularly from parietal bone, are derived from mesodermal origin, while cells in alveolar process are derived from neural crest cells [30, 31]. The different origins of cells also affect cell behaviors, including osteogenic differentiation ability. Second, the different mutations could cause different alteration of *DSPP* function, leading to different degree of cell response. The influences of *Dspp* null cells which completely lack of *Dspp* could be more potent than our mutation. Lastly, it was reported that *DSPP* processing was regulated by the internal ribosomal entry site [32]. This internal ribosomal entry site activity was varied among human embryonic kidney cell line, murine pre-osteoblast cell line, and rat odontoblast cell line [32]. Together, these evidences indicate that *DSPP* regulating cell behaviors could depend on types of cells and mutations. Future investigations on the effects of specific *DSPP* mutations on particular cell types would be beneficial to clarify molecular roles of *DSPP*.

It was hypothesized that delayed cell spreading may influence other phenotypes in *DSPP* mutant cells. Previous reports showed that cellular mechanotransduction, actin cytoskeleton, attachment, and spreading could influence other biological functions of the cells including osteogenic marker gene expression and extracellular matrix synthesis [33, 34]. Disruption of actin polymerization and formation of stress fiber were shown to decrease the expression of *ALP* in human bone cells and mineral deposition [35, 36]. Increased tension of actin cytoskeleton could enhance osteogenic differentiation [13]. In addition, enhancement of actin polymerization and traction forces in murine mesenchymal stem cells was shown to increase osteogenic differentiation [19]. Together, these evidences suggest the important role of cell spreading and actin formation/arrangement on osteogenic differentiation potency. In the present study, the delayed formation of stress fiber was observed in our mutant cells and the *ALP* mRNA level in the mutant cells was not upregulated compared to the significant increase of *ALP* level in the control upon cultured in osteogenic induction medium at day 7 compared to day 3. These findings imply that *DSPP* is engaged in/relates to osteogenic differentiation via mechanisms involving cell spreading and actin polymerization/arrangement.

In conclusion, our study identified the mutation, c.50C > T, p.P17L, in the exon 2 of the *DSPP* gene, localized in the DSP domain. We demonstrate for the first time that the *DSPP* alveolar bone cells isolated from a DGI patient exhibit compromised cell proliferation, colony formation, cell spreading, formation of stress fiber, and altered expression of *ALP*, *COL1*, and *OCN*, compared to the control cells isolated from healthy

donors. Our results support that the P17 residue of *DSPP* is a mutational hot spot and the DSP serves a critical function in bone homeostasis. Compromised characteristics of alveolar bone cells and dentin associated with *DSPP* mutation may contribute in the progression of endodontic-periodontic lesions commonly found in our DGI patients. The identification of pathogenic variants would therefore enable the definite diagnosis and proper management for the patients affected with DGI.

Acknowledgements We thank Pimsupa Kitsricharoenchai for providing the dental treatment for the proband.

Funding information This study was supported by the Thailand Research Fund (TRF) and Office of Higher Education Commission (OHEC) Thailand (MRG6080001), the Chulalongkorn Academic Advancement Into Its 2nd Century Project. Nunthawan Nowwarote is supported by the Ratchadapisek Sompot Fund for Postdoctoral Fellowship, Chulalongkorn University.

Compliance with ethical standards

Conflict of interest The authors declare that they have no conflict of interest.

Ethical approval All procedures performed in studies involving human participants were in accordance with the ethical standards of the institutional and/or national research committee and with the 1964 Helsinki declaration and its later amendments or comparable ethical standards.

Informed consent Informed consent was obtained from all individual participants included in the study.

References

- Suzuki S, Haruyama N, Nishimura F, Kulkarni AB (2012) Dentin sialophosphoprotein and dentin matrix protein-1: two highly phosphorylated proteins in mineralized tissues. *Arch Oral Biol* 57:1165–1175. <https://doi.org/10.1016/j.archoralbio.2012.03.005>
- Barron MJ, McDonnell ST, Mackie I, Dixon MJ (2008) Hereditary dentine disorders: dentinogenesis imperfecta and dentine dysplasia. *Orphanet J Rare Dis* 3:31. <https://doi.org/10.1186/1750-1172-3-31>
- de La Dure-Molla M, Philippe Fournier B, Berdal A (2014) Isolated dentinogenesis imperfecta and dentin dysplasia: revision of the classification. *Eur J Hum Genet* 23:445–451. <https://doi.org/10.1038/ejhg.2014.159>
- Kim J-W, Nam S-H, Jang K-T, Lee S-H, Kim C-C, Hahn S-H, JC-C H, Simmer JP (2004) A novel splice acceptor mutation in the *DSPP* gene causing dentinogenesis imperfecta type II. *Hum Genet* 115:248–254. <https://doi.org/10.1007/s00439-004-1143-5>
- Prasad M, Butler WT, Qin C (2010) Dentin sialophosphoprotein in biomineralization. *Connect Tissue Res* 51:404–417. <https://doi.org/10.3109/03008200903329789>
- Qin C, Brunn JC, Cadena E, Ridall A, Tsujigiwa H, Nagatsuka H, Nagai N, Butler WT (2002) The expression of dentin sialophosphoprotein gene in bone. *J Dent Res* 81:392–394. <https://doi.org/10.1177/154405910208100607>
- Chen Y, Zhang Y, Ramachandran A, George A (2016) *DSPP* is essential for normal development of the dental-craniofacial complex. *J Dent Res* 95:302–310. <https://doi.org/10.1177/0022034515610768>
- Gibson MP, Zhu Q, Liu Q, D'Souza RN, Feng JQ, Qin C (2013) Loss of dentin sialophosphoprotein leads to periodontal diseases in mice. *J Periodontol Res* 48:221–227. <https://doi.org/10.1111/j.1600-0765.2012.01523.x>
- Gibson MP, Jani P, Liu Y, Wang X, Lu Y, Feng JQ, Qin C (2013) Failure to process dentin sialophosphoprotein into fragments leads to periodontal defects in mice. *Eur J Oral Sci* 121:545–550. <https://doi.org/10.1111/eos.12088>
- Verdelis K, Ling Y, Sreenath T, Haruyama N, MacDougall M, van der Meulen MC, Lukashova L, Spevak L, Kulkarni AB, Boskey AL (2008) *DSPP* effects on in vivo bone mineralization. *Bone* 43:983–990. <https://doi.org/10.1016/j.bone.2008.08.110>
- Gu S, Liang J, Wang J, Liu B (2013) Histone acetylation regulates osteodifferentiation of human dental pulp stem cells via *DSPP*. *Front Biosci (Landmark Ed)* 18:1072–1079
- Wan C, Yuan G, Luo D, Zhang L, Lin H, Liu H, Chen L, Yang G, Chen S, Chen Z (2016) The dentin sialoprotein (DSP) domain regulates dental mesenchymal cell differentiation through a novel surface receptor. *Sci Rep* 6:29666. <https://doi.org/10.1038/srep29666>
- Kelly DJ, Jacobs CR (2010) The role of mechanical signals in regulating chondrogenesis and osteogenesis of mesenchymal stem cells. *Birth Defects Res C Embryo Today* 90:75–85. <https://doi.org/10.1002/bdrc.20173>
- Pornaveetus T, Srichomthong C, Suphapeetipom K, Shotelersuk V (2017) Monoallelic *FGFR3* and Biallelic *ALPL* mutations in a Thai girl with hypochondroplasia and hypophosphatasia. *Am J Med Genet A* 173:2747–2752. <https://doi.org/10.1002/ajmg.a.38370>
- Sukarawan W, Nowwarote N, Kerdpon P, Pavasant P, Osathanon T (2014) Effect of basic fibroblast growth factor on pluripotent marker expression and colony forming unit capacity of stem cells isolated from human exfoliated deciduous teeth. *Odontology* 102:160–166. <https://doi.org/10.1007/s10266-013-0124-3>
- Osathanon T, Sawangmake C, Ruangchainicom N, Wutikomwipak P, Kantukiti P, Nowwarote N, Pavasant P (2016) Surface properties and early murine pre-osteoblastic cell responses of phosphoric acid modified titanium surface. *J Oral Biol Craniofac Res* 6:2–9. <https://doi.org/10.1016/j.jobcr.2015.12.005>
- Lumbikanonda N, Sammons R (2001) Bone cell attachment to dental implants of different surface characteristics. *Int J Oral Maxillofac Implants* 16:627–636
- Osathanon T, Bessinyowong K, Arksornnukit M, Takahashi H, Pavasant P (2011) Human osteoblast-like cell spreading and proliferation on Ti-6Al-7Nb surfaces of varying roughness. *J Oral Sci* 53:23–30. <https://doi.org/10.2334/josnurd.53.23>
- Seo CH, Jeong H, Feng Y, Montagne K, Ushida T, Suzuki Y, Furukawa KS (2014) Micropit surfaces designed for accelerating osteogenic differentiation of murine mesenchymal stem cells via enhancing focal adhesion and actin polymerization. *Biomaterials* 35:2245–2252. <https://doi.org/10.1016/j.biomaterials.2013.11.089>
- Lee SK, Lee KE, Song SJ, Hyun HK, Lee SH, Kim JW (2013) A *DSPP* mutation causing dentinogenesis imperfecta and characterization of the mutational effect. *Biomed Res Int* 2013:948181–948187. <https://doi.org/10.1155/2013/948181>
- Xiao S, Yu C, Chou X, Yuan W, Wang Y, Bu L, Fu G, Qian M, Yang J, Shi Y, Hu L, Han B, Wang Z, Huang W, Liu J, Chen Z, Zhao G, Kong X (2001) Dentinogenesis imperfecta 1 with or without progressive hearing loss is associated with distinct mutations in *DSPP*. *Nat Genet* 27:201–204. <https://doi.org/10.1038/84848>
- Jaha H, Husein D, Ohyama Y, Xu D, Suzuki S, Huang GT, Mochida Y (2016) N-Terminal dentin sialoprotein fragment induces type I collagen production and upregulates dentinogenesis marker expression in osteoblasts. *Biochem Biophys Res* 6:190–196. <https://doi.org/10.1016/j.bbrep.2016.04.004>
- Marolt D, Rode M, Kregar-Velikonja N, Jeras M, Knezevic M (2014) Primary human alveolar bone cells isolated from tissue

- samples acquired at periodontal surgeries exhibit sustained proliferation and retain osteogenic phenotype during in vitro expansion. *PLoS One* 9:e92969. <https://doi.org/10.1371/journal.pone.0092969>
24. Kim J-W, Hu JC-C, Lee J-I, Moon S-K, Kim Y-J, Jang K-T, Lee S-H, Kim C-C, Hahn S-H, Simmer JP (2005) Mutational hot spot in the DSPP gene causing dentinogenesis imperfecta type II. *Hum Genet* 116:186–191. <https://doi.org/10.1007/s00439-004-1223-6>
 25. Fawzy El-Sayed KM, Boeckler J, Dorfer CE (2017) TLR expression profile of human alveolar bone proper-derived stem/progenitor cells and osteoblasts. *J Craniomaxillofac Surg* 45:2054–2060. <https://doi.org/10.1016/j.jcms.2017.09.007>
 26. Gibson MP, Zhu Q, Wang S, Liu Q, Liu Y, Wang X, Yuan B, Ruest LB, Feng JQ, D'Souza RN, Qin C, Lu Y (2013) The rescue of dentin matrix protein 1 (DMP1)-deficient tooth defects by the transgenic expression of dentin sialophosphoprotein (DSPP) indicates that DSPP is a downstream effector molecule of DMP1 in dentinogenesis. *J Biol Chem* 288:7204–7214. <https://doi.org/10.1074/jbc.M112.445775>
 27. Gibson MP, Jani P, Wang X, Lu Y, Qin C (2014) Overexpressing the NH(2)-terminal fragment of dentin sialophosphoprotein (DSPP) aggravates the periodontal defects in Dspp knockout mice. *J Oral Biosci* 56:143–148. <https://doi.org/10.1016/j.job.2014.06.003>
 28. Ozer A, Yuan G, Yang G, Wang F, Li W, Yang Y, Guo F, Gao Q, Shoff L, Chen Z, Gay IC, Donly KJ, MacDougall M, Chen S (2013) Domain of dentine sialoprotein mediates proliferation and differentiation of human periodontal ligament stem cells. *PLoS One* 8:e81655. <https://doi.org/10.1371/journal.pone.0081655>
 29. Jia J, Bian Z, Song Y (2015) Dspp mutations disrupt mineralization homeostasis during odontoblast differentiation. *Am J Transl Res* 7:2379–2396
 30. Chai Y, Jiang X, Ito Y, Bringas P Jr, Han J, Rowitch DH, Soriano P, McMahon AP, Sucov HM (2000) Fate of the mammalian cranial neural crest during tooth and mandibular morphogenesis. *Development* 127:1671–1679
 31. Jiang X, Iseki S, Maxson RE, Sucov HM, Morriss-Kay GM (2002) Tissue origins and interactions in the mammalian skull vault. *Dev Biol* 241:106–116. <https://doi.org/10.1006/dbio.2001.0487>
 32. Zhang Y, Song Y, Ravindran S, Gao Q, Huang CC, Ramachandran A, Kulkarni A, George A (2014) DSPP contains an IRES element responsible for the translation of dentin phosphophoryn. *J Dent Res* 93:155–161. <https://doi.org/10.1177/0022034513516631>
 33. Schwartz MA (2009) The force is with us. *Science* 323:588–589. <https://doi.org/10.1126/science.1169414>
 34. Titushkin I, Cho M (2007) Modulation of cellular mechanics during osteogenic differentiation of human mesenchymal stem cells. *Biophys J* 93:3693–3702. <https://doi.org/10.1529/biophysj.107.107797>
 35. Goncharenko AV, Malyuchenko NV, Moisenovich AM, Kotlyarova MS, Arkhipova AY, Kon'kov AS, Agapov II, Molochkov AV, Moisenovich MM, Kirpichnikov MP (2016) Changes in morphology of actin filaments and expression of alkaline phosphatase at 3D cultivation of MG-63 osteoblast-like cells on mineralized fibroin scaffolds. *Dokl Biochem Biophys* 470:368–370. <https://doi.org/10.1134/S1607672916050197>
 36. Rodriguez JP, Gonzalez M, Rios S, Cambiasso V (2004) Cytoskeletal organization of human mesenchymal stem cells (MSC) changes during their osteogenic differentiation. *J Cell Biochem* 93:721–731. <https://doi.org/10.1002/jcb.20234>